Lightning Flash Observations on a Wind Turbine in Croatia: Insights from Current Measurements, High-Speed Camera, LLS and Lightning Imager Data

F. Vukovic, J. Montanyà, B. Filipovic-Grcic

***Abstract*--This study presents a comprehensive analysis of lightning activity at a wind farm lightning observatory in Croatia, where lightning strikes on a wind turbine are monitored using synchronized current measurements, high-speed optical recordings, and lightning location system (LLS) data. With the recent launch of the Meteosat Third Generation (MTG) Lightning Imager (LI) in July 2024, continuous optical radiance data is also available. By leveraging precise timestamps, LI radiance data is correlated with ground-based measurements. During the period, the current measurement system detected nine events serving as ground truth and, for some events, being complemented by high-speed camera data for LLS and LI. Ground-based equipment consistently validates each other in stroke detection, and current measurements of continuing-type currents are further corroborated by HS camera data and extracted luminance profiles. The LI detected all nine flashes at the instrumented WT. In every flash, LI detections preceded the currents measured at the WT, suggesting that the leaders and strokes were triggered by in-cloud lightning activity. LI also confirmed the polarity of the involved lightning leaders, enabled more precise quantification of flash parameters such as duration and extension, and verified the presence of continuing currents.**

***Keywords*: wind turbine; initial continuous current; upward lightning; lightning imager; Rogowski coils; high-speed camera**

I. Introduction

The Croatian wind farm (WF) lightning observatory monitors lightning activity in a wind farm using LLS data and, since 2022, through a lightning current waveform measurement system (LCWMS) installed on a single 3 MW wind turbine in southern Croatia. The WF area is characterized by medium to high winter lightning activity, as indicated by meteorological data and LLS-based maps ([1]). Before its installation, the LCWMS was tested in the high-voltage laboratory at the Faculty of Electrical Engineering and Computing, University of Zagreb [2]. In 2023, a high-speed (HS) camera was also integrated into the system to validate current measurements and provide additional insights into lightning flash attachment, channel evolution, and flash progression. The camera was similarly tested in the high-voltage laboratory prior to its deployment [3]. To date, current waveforms have been recorded for about 200 lightning events, with HS camera footage available for several dozens of these events. Preliminary results from high-frequency (HF), which is optimized to measure up to 1 MHz, and low-frequency (LF) Rogowski coil, which is optimized to measure up to 10 kHz, measurements were presented in [4]. In [4] recurring issues were identified, including 2 MHz oscillations in HF sensor recordings and DC offsets in LF sensor data. Regarding camera recordings, some videos clearly show lightning channels, while others are partially obscured due to cloudy or misty conditions. Furthermore, in prior work [5] involving LCWMS and HS camera measurements, several lightning events were successfully correlated with LLS data.

This lightning observatory facility is unique in Europe as it conducts long-term lightning observations on a WT in winter lightning activity area. Comparable current measurement studies have been conducted only in Japan, where instrumented WTs have been used. These include investigations under the New Energy and Industrial Technology Development Organization (NEDO) project [6], studies carried out by Mitsubishi Heavy Industries, Ltd. (MHI) [7], and research conducted at the Nikaho Kogen wind farm (WF) by Electric Power Development Co., Ltd. (J-Power) and the Central Research Institute of Electric Power Industry (CRIEPI) [8]. In all the aforementioned investigations in Japan, current measurements were performed using a single Rogowski coil, installed at the base of the tower, often in combination with one or more conventional-speed cameras, across multiple wind farms and WTs.

Newer investigations on WTs include HS imaging investigations of lightning on WTs [9], [10], combination of HS imaging and current measurement [11], [12] and high-speed imaging and ground-based sensors [13]. On tall towers, HS optical observations have rich operational experience in conjunction with measuring lightning currents and additional lightning monitoring equipment such as local E-field, B-Field sensors and X-ray sensors or large scale systems such as national lightning location systems [14]-[25].

Significant efforts have also been made in space-based observations of lightning [26], [27] and their applications in power systems [28]. In [28] the authors discuss the use of space-based optical lightning detection in several critical areas, including the identification of initial continuous currents (ICCs) at the onset of upward flashes, the detection of

This work was supported by the Croatian Science Foundation (HRZZ, DOK-2021-02) and European Regional Development Fund within project DESMe, KK 01.1.1.07.0028.

F. Vukovic and B. Filipovic-Grcic are with the University of Zagreb Faculty of Electrical Engineering and Computing, Croatia (e-mail: franjo.vukovic@fer.hr, bozidar.filipovic-grcic@fer.hr).
J. Montanyà is with Polytechnic University of Catalonia, Spain (e-mail: joan.montanya@upc.edu).
Paper submitted to the International Conference on Power Systems Transients (IPST2025) in Guadalajara, Mexico, June 8-12, 2025.

continuing currents (CCs) occurring in later stages, the observation of upward-triggered lightning flashes (e.g., positive cloud-to-ground (CG) flashes that initiate upward lightning), and the assessment of lightning exposure risks for overhead transmission lines and the broader impact on power systems. Since July 2024, the LI onboard the MTG satellite has been providing continuous, real-time space-based lightning detection by capturing optical signals from lightning activity. The LI monitors lightning occurrence over Europe, Africa, and South America from geostationary orbit. This study integrates LI data with data from the Croatian WF lightning observatory to cross-validate the measurements and offer complementary perspectives on lightning phenomena.

II. Instrumentation at Wind Farm Lightning Observatory and MTG LI specifications

Figure 1 illustrates the site map, showing the relative positions and elevations of the substation with the HS camera and WTG4, where the LCWMS is installed. The HS camera is located at the substation. The substation is located at an elevation of approximately 757 meters, while the wind WT equipped with the lightning current waveform measurement system is positioned on a hill 3.5 kilometers away at an elevation of 1250 meters. The camera is set to be triggered by the LCWMS system. The camera records with 24000 fps for approximately 1 s.

Both the LF and HF sensors are Rogowski coils connected to an integrator via a coaxial cable. The LF sensor was installed to measure continuing-type currents, such as initial ICCs, with an optimal measurement range of up to ±12.5 kA. However, the LF sensor is connected to a digitizer that saturates at 10 volts. Given the sensor's sensitivity coefficient (0.6 mV/A), this corresponds to an approximate upper limit of 18 kA [2], which will be relevant for later analysis of results. As for the HF sensor, it captures currents up to ±250 kA [2], although such high amplitudes are extremely rare in Croatia. According to LLS data from the past few years, the average stroke amplitude is lower than 10 kA. The HF sensor is used to measure pulse-type currents.

The system has recorded approximately 200 lightning events, the vast majority of which exhibit a clearly present ICC, indicating that they are of the upward type. However, there are several events in which an ICC does not appear to be present, leading the authors to believe they may be of the downward type. It must be noted, however, that without absolute visual confirmation from the high-speed camera, it cannot be claimed with 100% certainty that these events are downward flashes, as the LF sensor may not have been able to properly register the ICC in those cases.

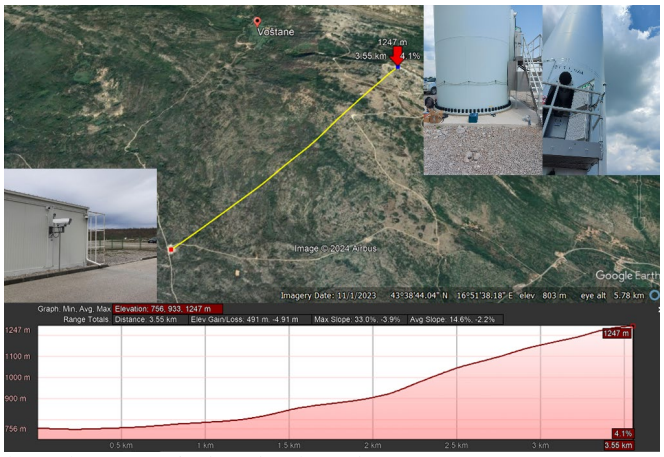

Fig. 1. Site map: 110/20 kV substation and WTG4

The LLS data is also available for the site. On a weekly basis, registered lightning flashes in the WT area are spatially correlated with specific WTs in the WF based on their collection areas. The collection area is determined according to the IEC standard [29] based on the effective structure height. For all WTs in the WF, the maximum structure height, when one blade is aligned with the tower, is 132 m, resulting in a collection area with a radius of 400 m (3 x 132 m). When a lightning flash registered by the LLS corresponds to a point inside this radius, it is deemed that the lightning flash has hit the WT.

In addition to information from the LLS, since July 4th, the Lightning Imager (LI) onboard the 3rd generation of the Meteosat (MTG) I1 satellite [33], [36] has been providing data on the detection time, location, and intensity (narrowband at 777.4 nm) of optical emissions from lightning flashes. The LI mainly detects the luminosity from lightning scaping from clouds after scattering and absorption with cloud particles. So, LI detects luminosity from total lightning: intra-cloud and CG. The LI composite field-of-view of the four optical cameras includes Africa, Europe, and part of the Atlantic Ocean, with a spatial resolution of 4.5 km at the equator and ~7 km in Croatia. LI sampling time (exposure time) is 1 ms. This work uses LI level 2 group data, and correction for parallax and photon travel has been applied. In this work, we use public LI level 2 lightning groups (LGR) data. LI groups will be used to provide a plan view (lat-lon) of the flashes as well as the time-distance representation of flashes. Based on [35] and [31], the time of occurrence of each LI group and its horizontal distance to the location of the wind turbine (WTG4 is the reference, 0 km) will be plotted in the time-distance plot. As shown in [35] and [31], the alignment of the points in the time-distance plot is associated to negative or positive leader development according to the slope (dashed lines, e.g. Figure 3b and 6b). The slopes of the refence lines (dashed lines) correspond to speed of typical negative leader propagation:$1 \times 10^5\ m\ s^{-1}$ to $1 \times 10^6\ m\ s^{-1}$ and of typical positive leader propagation: $2 \times 10^4\ m\ s^{-1}$

Additionally, from the LI groups of a flash, the integrated optical radiance will be calculated by integrating the radiance of all the groups during each 1 ms exposure frame [28]. The integrated radiance will be compared with the measured

current and high-speed video measurements. In addition, the integrated radiance is also used to intensify the presence of continuous luminosity, which is commonly related to continuing currents (e.g., [28]).

III. Results

In this section flashes to WTG4 are analyzed between July 20 and October 5, 2024. This period corresponds to the first public LI data streaming. Nine lightning events on WTG4 were detected during this period, including downward negative flashes, positive upward flashes containing only ICC, negative upward flashes containing only ICC, and upward positive flashes containing both ICC and pulse-type currents.

On July 20, 2024, three flashes containing downward negative CG strokes were recorded at WTG4. These flashes occurred at 10:00:49.844, 10:01:27.240, and 10:01:51.920 UT. The first flash consisted of a single stroke, the second comprised eight strokes, and the third included five strokes. For the first two flashes, the camera data is available, however there is no clear view of the channel because of the poor visibility conditions. For this specific case, it seems that cloud cover or fog is blocking the view across the entire frame. However, during the times of strokes, there are global changes in brightness across the entire screen. The luminance profiles were calculated by determining the average pixel intensity of each frame and properly timestamping it. These luminance profiles serve only to temporally confirm the LLS and LF/HF sensor measurements.

Figure 2 illustrates the LF and HF sensor current measurement as well as HS camera luminance profile overlapping together for the first negative CG flash that contained single stroke and occurred at 10:00:49.844 UT. The vertical dashed line represents the time of stroke that LLS detected in the collection area of WTG4. The LLS registered a peak current of 24 kA, while the HF sensor measured ~37 kA. Note that the LF sensor saturates at 18 kA. In the figure, the extracted luminance has been scaled down by a specific factor to facilitate easier comparison with the current waveform. The scaling factor was chosen based on the maximum amplitude of the LF sensor current and the maximum luminosity value to clearly indicate their temporal correlation visually. Each data source for the stroke that hit the WT aligns within a millisecond.

The camera also captured luminance from nearby lightning activity, as shown in the figure. In this particular case, the LLS located nearby lightning activity outside the WT collection area, indicating that the associated strokes struck the nearby soil. Additionally, this activity was not captured by the LCWMS, which serves as the ground truth.

Similar observations apply to the other two negative CG flashes, both of which contained multiple strokes. For each stroke in these two events, which the authors believe to be downward flashes, LF and HF sensor and LLS-detected strokes correlated within an about a millisecond. In the case of the second flash, which started around 10:01:27.240 and contained eight strokes, the LLS did not detect two of them. Additionally, two detected strokes were located just outside the WT collection area and were classified as cloud-to-cloud discharges. As in the first analyzed case, there is no clear view of the lightning channel. However, the extracted luminosity profile suggests that only the first three strokes can be identified, and they overlap with those captured by the LF and HF sensor. For the third flash event, which started around 10:01:51.920, both the LF and HF sensor detected five stroke events that also correlated well with the LLS strokes. However, the LLS located two of these strokes outside the WT collection area and classified them as cloud-to-cloud discharges. In this case, no HS camera footage is available, as the memory buffer was full due to consecutive camera triggers.

Figure 3 presents the LI detections of the first flash at 10:00:49.844 UT. The locations of the LI groups in Figure 3a show two distinct clusters. One is close to WTG4 (black circle), and the other is ~25 km to the south. The time-distance plot in Figure 3b displays the time and distance sequence of the LI groups in the flash.

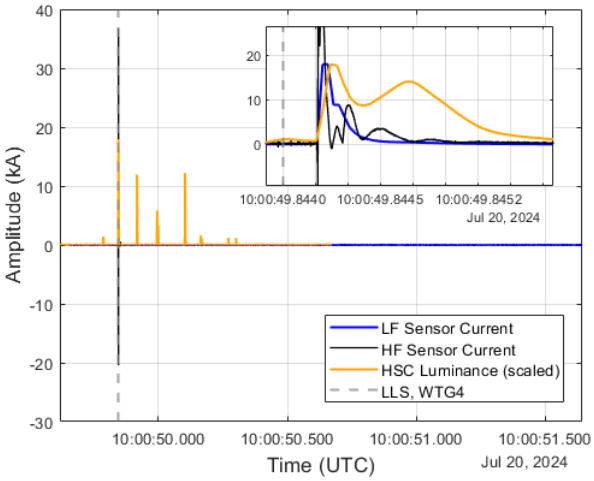

Fig. 2. Flash on 20/07/2024 at 10:00:49.844 UT. Measured lightning current by the LF (blue) and HF (black) sensors at WTG4, HS camera luminance profile scaled (orange) and CG stroke LLS detection (vertical dashed line).

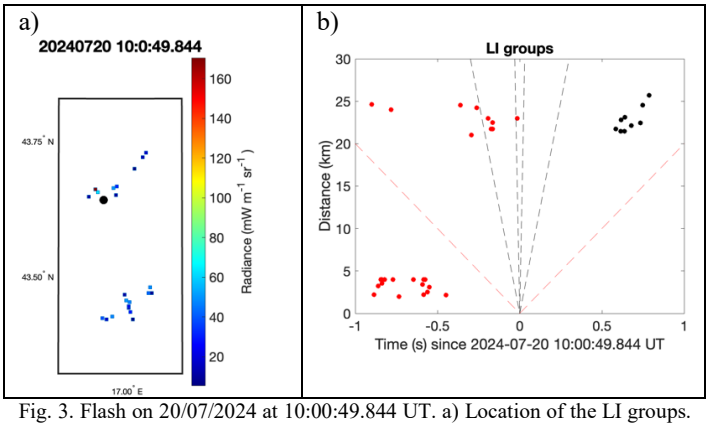

Fig. 3. Flash on 20/07/2024 at 10:00:49.844 UT. a) Location of the LI groups. The wind turbine is represented as a black filled circle). b) Time distance plot. The location of WTG4 is the distance origin (0 km) whereas the time 0 s corresponds to the lightning current measurement at the same wind turbine. Red and black dots correspond to the LI groups detected before the current measured before and after at the wind turbine, respectively. The dashed lines are references for speed for typical negative leader propagation: $1 \times 10^5\ m\,s^{-1}$ to $1 \times 10^6\ m\,s^{-1}$ and for typical positive leader propagation: $2 \times 10^4\ m\,s^{-1}$.

In this plot, the location of WTG4 is set as the spatial origin, and the time 0 s corresponds to the time of the measured stroke current. The time-distance plot reveals that the LI groups close to WTG4 occurred -0.5 s before with some activity between -0.5 s and the stroke time (0 s) at ~25 km (south cluster). At the time of the stroke, no LI groups were detected. About 0.5 s after the stroke, LI detections occurred in the south cluster ~25 km.

Figure 4 depicts the LI-integrated optical radiance of the flash and the measured current at WTG4. Note that LI does not contain any detections at the time of the measured current despite the stroke amplitude being approximately 37 kA, as measured by the HF sensor, and approximately 24 kA, as reported by the LLS. A LI detection is found 15 ms before at ~25 km (Figure S2b in the Supporting Information).

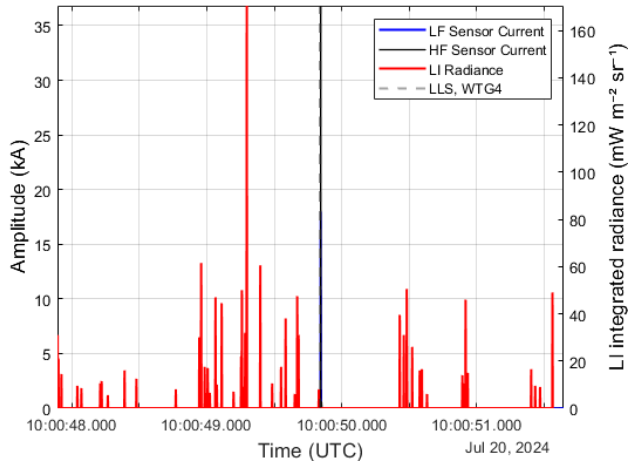

Fig. 4. Flash on 20/07/2024 at 10:00:49.844 UT. Measured lightning current by the LF (blue) and HF (black) sensors at WTG4, integrated LI optical radiance (red), and CG stroke LLS detection (vertical dashed line).

A similar pattern is found in the other two flashes occurring during the same day in Figures S3-S6 in the Supporting Information.

On August 3 and August 19, 2024, the measured currents of the flashes at WTG4 presented only negative ICC from upward positive leaders. These two cases present some common features which will be described next. For both cases, LF sensor and HS camera data are available. Figure 5 shows the August 3 negative ICC current measurement, with the scaled luminosity profile overlapped. According to the LF sensor, the flash started on August 3 around 00:47:20.440 UT, reached approximately 74 amps, and lasted about 160 ms. Figure 5 also includes an HS camera frame where the lightning channel is visible. For the August 19 lightning flash, which occurred around 10:55:32.330 UT and lasted about 100 ms with a peak amplitude of 60 amps, no visible lightning channel is present in the HS camera frames. However, the luminosity profile is extracted and more or less overlaps with the LF sensor current (not shown here). As expected, the LLS system is blind to flashes that lack pulse-type currents, such as strokes. Consequently, no data are available for either August case within the collection area of WTG4 at that time.

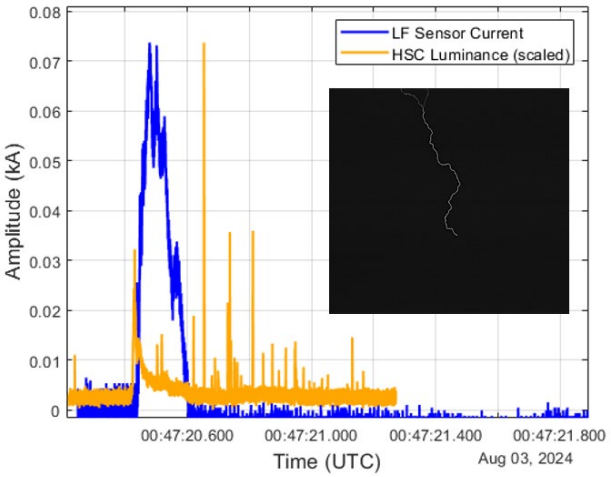

Fig. 5. Flash on 03/08/2024 at 00:47:20.437 UT. Measured lightning current by the LF (blue) sensor at WTG4 and HS camera luminance profile scaled (orange) with HS camera frame containing visible lightning channel.

LI groups of August 3, 2024 at 00:47:20.437 UT flash are shown Figure 6. According to Figure 6b, the flash started at ~70 km from WTG4 and propagated towards the wind turbine. The LI groups (in red) before the current measured at WTG4 suggest slow negative leader propagation at $\sim 1 \times 10^5\ m\ s^{-1}$ for the LI groups between -0.5 s to -0.2 s and fast negative leader development $\sim 1 \times 10^6\ m\ s^{-1}$ for the LI groups between -0.1 s to the time of the upward leader at WTG4. See caption in Fig. 3 and Fig. S7 (supporting information) for the interpretation of the leader speeds based on the slopes (dashed lines) in the time-distance plots.

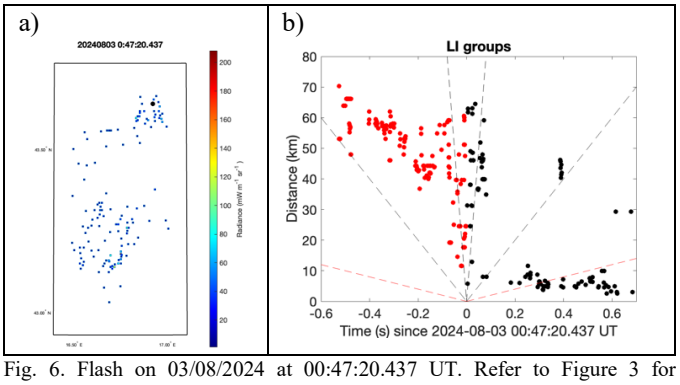

Fig. 6. Flash on 03/08/2024 at 00:47:20.437 UT. Refer to Figure 3 for explanation

Figure 7 presents the LI optical radiance and the measured current. Note that LI provided detections until the measured ICC peaked. These detections correspond to the ones that extend to ~65 km between 0 s and ~0.1 s in Figure 6b. After 0.2 s, corresponding to the time the ICC vanishes, positive leader development at the wind turbine location is identified in the LI groups from 0.2 to ~0.6 s in Figure 6b. The plots for the flash on August 19, 2024 (Figures S9-S10 in Supporting Information) suggest a similar pattern to the described flash.

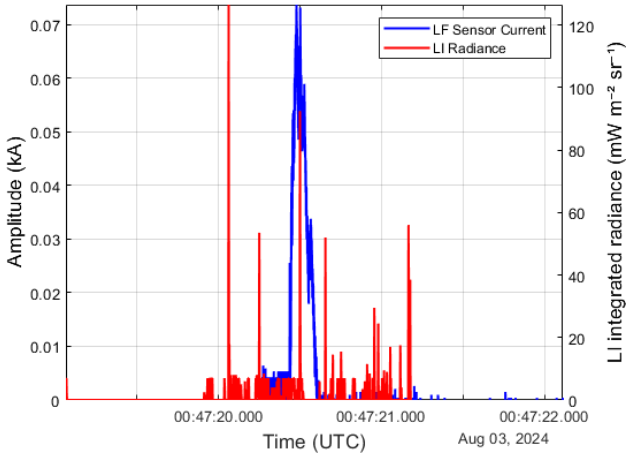

Fig. 7. Flash on 03/08/2024 at 00:47:20.437 UT. Measured lightning current by the LF (blue) sensor at WTG4 and integrated LI optical radiance (red)

Two upward positive flash events that only contained ICC, associated with upward negative leaders, from WTG4 were measured on September 13, 2024. Only LF sensor data are available for both cases, and no accompanying camera video is available. Additionally, there are no HF current sensor or LLS records, as expected. According to the LF sensor data, the first flash started around 02:49:42.334 UT, lasted approximately 150 ms, and reached a peak current of about 481 A. The second flash occurred at 02:53:16.838 UT, lasted around 70 ms, and had a peak amplitude of 1.29 kA.

Figures 8 and 9 present the LI detections associated with the flash at 02:53:16.838 UT. The flash started -0.2 s before the current measured at WTG4, producing continuous LI groups (red dots) from a horizontal distance of ~15 km (WTG4 as reference) propagating at positive leader speed (Figure 8b, Figure 9 and Figure S13 in the supporting information). Some negative leader development can also be identified from the LI groups (red) approaching the turbine before the inception of the leader at WTG4.

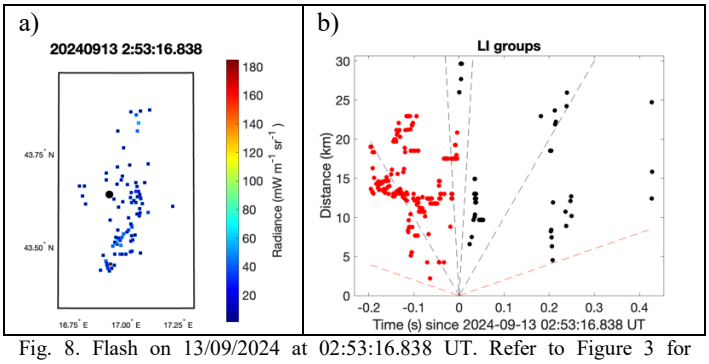

Fig. 8. Flash on 13/09/2024 at 02:53:16.838 UT. Refer to Figure 3 for explanation.

The continuous luminosity of the flash before the initiation of the upward negative leader at WTG4 is clearly seen in Figure 9. The luminosity (red signal in Figure 9) remains almost continuous from the beginning of the flash until the current is measured at the wind turbine (blue signal in Figure 7). The same is observed in the flash at 02:49:42.334 UTC (Figures S12-S13 in the Supporting Information).

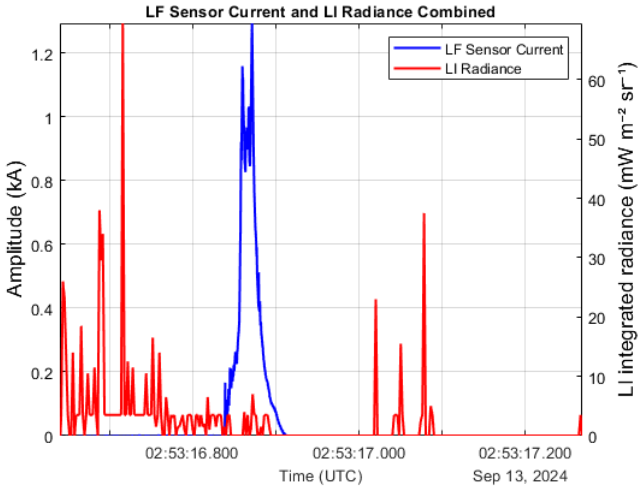

Fig. 9. Flash on 13/09/2024 at 02:53:16.838 UT. Measured lightning current by the LF (blue) sensor at WTG4 and integrated LI optical radiance (red).

Two upward positive flashes to WTG4 were observed on October 5, 2024. The first flash occurred at 14:59:31.633 UT (a single return stroke), while the second occurred a couple of minutes later at 15:03:16.207 UT (two return strokes). The provided timings correspond to the first return stroke of each flash. For both events, HS camera recordings captured visible lightning channels, including the upward leader development. Figure 10 presents the LF and HF sensor current measurements, and the HS camera luminance profile overlaid for the first flash at 14:59:31.633 UT. A vertical dashed line marks the return stroke timing detected by the LLS within the WTG4 collection area. The LLS registered a peak current of 113.9 kA, while the HF sensor recorded a peak current of approximately 200 kA. Notably, the ICC duration was extremely short, lasting around 2 ms, with no no-current period observed between the ICC and return strokes in the LF sensor data. The HS camera confirms this as an upward flash, as shown in Figure 11, which illustrates several nonconsecutive frames of upward leader development.

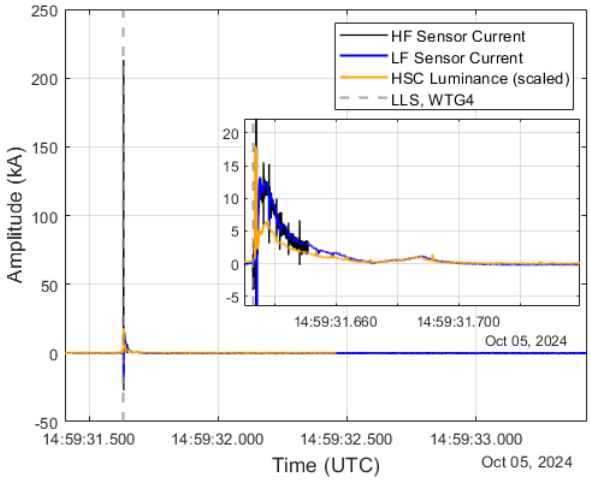

Fig. 10. Flash 05/10/2024 at 14:59:31.633 UT. Measured lightning current by the LF (blue) and HF (black) sensors at WTG4, HS camera luminance profile scaled (orange) and CG stroke LLS detection (vertical dashed line).

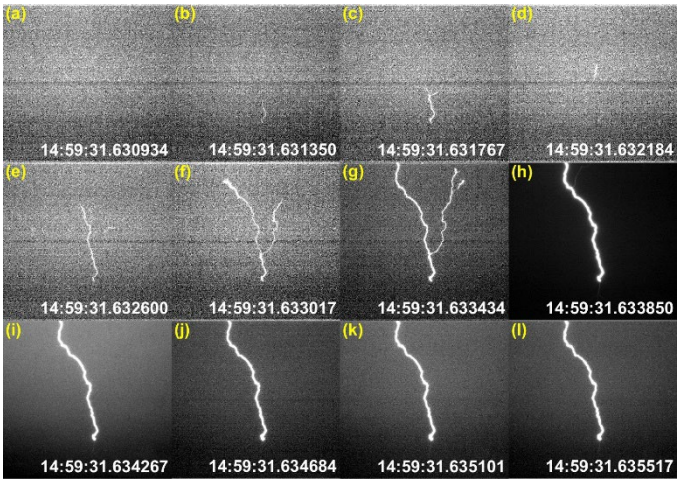

Fig. 11 Flash 05/10/2024 at 14:59:31.633 UT. HS camera frames show the upward leader development, which initiated at approximately 14:59:31.631.

Figures 12 and 13 correspond to the LI detections of the first flash. Both flashes started with LI groups (red dots in Figure 12b and S17b) detected at ~4 km a few milliseconds before the wind turbine current measurement. In the case of the flash in Figure 12, the LI groups (black dots in Figure 12b) just after the current started at 0 s until 50 ms suggest the presence of negative leader propagation that might be related to the channel connected to the wind turbine and supplying some continuing current as seen in the current waveform (Figure 13).

The currents of the two positive upward flashes on October 5, 2024, started with large peak current strokes of ~200 kA (Figure 13) and ~90 kA (Figure S18) accompanied by LI optical radiance pulses. In the case of the flash in Figure S18, a subsequent positive stroke was not detected by the LI. According to the HF current sensor, the subsequent positive stroke contained an amplitude of ~30 kA.

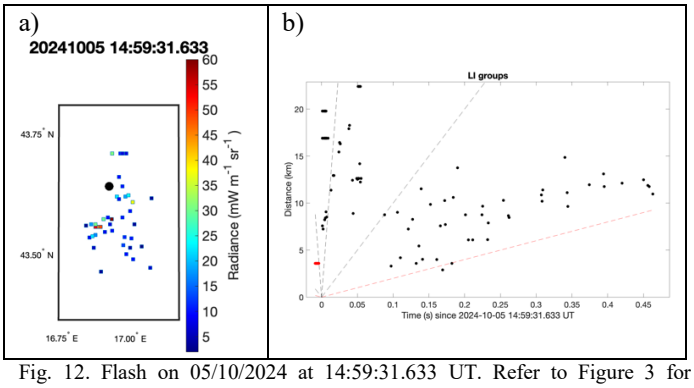

Fig. 12. Flash on 05/10/2024 at 14:59:31.633 UT. Refer to Figure 3 for explanation.

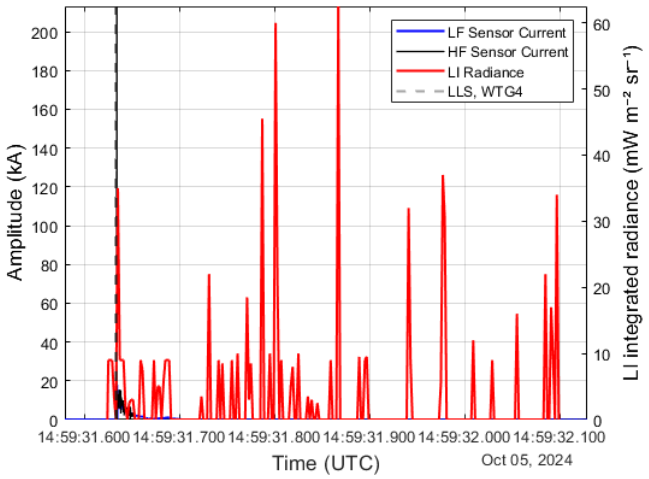

Fig. 13. Flash on 05/10/2024 at 14:59:31.633 UT. Measured lightning current by the LF (blue) and HF (black) sensors at WTG4, integrated LI optical radiance (red), and CG stroke LLS detection (vertical dashed line).

IV. Discussion Associated with LI

LI detected the nine measured flashes to WTG4 from July 20 to October 5, 2024. In general, LI detected groups before and after the currents were measured at the WT. The detection of LI groups before the currents measured at the WTs indicates that some in-cloud leader development triggers all the leaders and strokes at the WT. This is consistent with [30-31], where self-initiated lightning flashes are favored during winter-type thunderstorms because of their lower altitudes of the charge regions compared to more convective storms.

The three cases of downward negative -CG strokes at WTG4 on July 20, 2024, were preceded by some LI groups detected at the location of the WT between -0.5 s to -2 s before the strokes. In the three cases, a second cluster of LI groups is detected at a distance beyond ~20 km from the WT. LI did not report the strokes to the WT, although some peak current reached several tens of kA. The lack of LI detections at the time of the strokes might be due to a low initiation altitude of those -CG strokes (e.g., at the low positive charge region of the thundercloud). In addition, the flash occurred during the daytime, during which the detection efficiency of space-based optical lightning detectors was reduced due to the background intensity [32], [33].

The cases of current events with only negative ICC related to upward positive leaders from WTG4 (August 2024 cases) can correspond to the lightning-triggered upward lightning (LTUL) case [34,28]. In these flashes, LI groups likely from in-cloud leaders propagating at negative leader speed towards the WT were found before measuring the currents. These are consistent with the LTUL mechanism in [34,28], where negative leaders remove positive charge aloft the WT, favoring the inception of upward positive leaders from the tall object. In the presented cases, large peaks of luminosity are found during the ICC corresponding to LI groups distant to the WT (LI groups in Figures 6 and S9 and integrated radiance in Figures 7 and S10).

Interestingly, the positive ICC current measurements at WTG4 on September 13 showed a similar pattern in the LI luminosity

signals. The positive ICC by negative upward leaders from the WT is preceded by a long period (>100 ms) of continuous LI detections. The continuous detections of LI groups have been associated with in-cloud positive leader development (Figure 8) that would favor the exposure of the WT to more intense negative electric fields due to the reduction of negative charge in the cloud [37]. The cloud top temperature analysis in Figure S19 in section S2 (Supporting Information) suggested that the WT was under a convective cell instead of a stratiform cloud.

In the two positive upward flashes on October 5, 2024, LI reported groups <20 ms before the positive +CG strokes at distances <5 km. The existence of previous in-cloud activity is supported by an increase in brightness seen in the high-speed video frames before the initiation of the upward leader. The time-distance analysis in the flash in Figure 12 suggests that after the +CG stroke, fast negative leader development in the cloud for ~15 ms is consistent with the duration of the visible channel after the stroke in the high-speed video. The cloud top temperature analysis in Figure S20 in section S2 (Supporting Information) indicates that the WT was under a stratiform region with a cloud top at ~6.4 km. In such a case, the stratiform region might have been positively charged, and some in-cloud breakdown favored triggering the upward negative leader from the WT [30].

V. Conclusions

This paper analyzes multiple lightning events on a WT during the summer and autumn of 2024. Based on onsite-measured waveforms, the lightning flashes were classified into four categories: downward negative flashes, positive upward flashes containing only ICC, negative upward flashes containing only ICC, and upward positive flashes containing both ICC and pulse-type currents.

The flashes were analyzed using data from LF and HF sensors installed locally (Rogowski coils and integrators), a high-speed camera operating at 24000 fps, LLS, and LI. Current measurements from HF and LF sensors, along with high-speed camera data, serve as the ground truth for both LLS and LI. All ground-based equipment is independently synchronized, and their measurements consistently temporally validate one another. CG strokes detected in current measurements are confirmed by LLS data in the area and by HS camera data. Continuing-type currents are corroborated by luminance profiles extracted from the camera data and from camera frames of leaders.

The LI has demonstrated the detection of the nine investigated flashes to the instrumented WT. In all the flashes, despite being of different types, we found preceding LI detections to the currents measured at the WT, suggesting that the leaders and strokes to the WT were triggered by in-cloud lightning activity. LI data allows us to identify the triggering modes of the different flashes. In the case of downward negative flashes, we found preceding LI detections at the location of the WT -0.5 s to -2 s before the strokes at the WT. In the case of measured negative ICC-only events, LI detections suggested that the upward leaders were initiated by approaching in-cloud negative, whereas in the cases of positive ICC-only, they were preceded by abundant LI detections presumably related to positive leader development in convective cores. In the rare cases of positive upward flashes with intense stroke currents, LI has shown some lightning activity shortly before initiating the upward positive leader from the turbine. Moreover, LI has detected some groups suggesting the propagation of negative leaders that might be related to the continuing current just after the positive stroke.

Optical space-based detection of lightning has been able to complement in-situ current measurements and LLS CG stroke data, enabling the identification of the polarity of the involved lightning leaders, the mode of triggering of the flash at the WT, better quantification of general parameters of the flash such as duration and extension; and the identification of the presence of continuing currents. On the contrary, we found that the LI failed on the detection at the time of some CG strokes. In future work, LI imager data could also be utilized for:

- fault correlation on overhead lines caused by lightning flashes, in conjunction with detection from the LLS data;
- estimation of lightning flash density along overhead line route;
- correlation with monitoring systems for recording overvoltages and transients in power system to confirm lightning caused overvoltages;
- identification of continuing currents which allows extending the lightning risk assessment to the contribution of energetic flashes - this can be important for selecting surge arresters‘ charge and energy capabilities.

VI. References

[1] J. F. V. March, J. Montanya, F. Fabro, O. van der Velde, D. Romero, G. Sola, M. Freijo, N. Pineda, Winter lightning activity in specific global regions and implications to wind turbines and tall structures, in: 2016 33rd International Conference on Lightning Protection (ICLP), IEEE, 2016: pp. 1–5. https://doi.org/10.1109/ICLP.2016.7791447.

[2] F. Vukovic, V. Milardic, D. Milos, B. Filipovic-Grcic, N. Stipetic, B. Franc, Development and laboratory testing of a lightning current measurement system for wind turbines, Electric Power Systems Research 223 (2023) 109572. https://doi.org/10.1016/j.epsr.2023.109572.

[3] F. Vukovic, V. Milardic, B. Filipovic-Grcic, N. Stipetic, B. Franc, D. Milos, Incorporating a High-speed Camera in the Lightning Current Measurement System for Wind Turbines, in: 2023 4th International Conference on Smart Grid Metrology (SMAGRIMET), IEEE, 2023: pp. 1–6. https://doi.org/10.1109/SMAGRIMET58412.2023.10128662.

[4] F. Vukovic, B. Filipovic-Grcic, N. Stipetic, B. Franc, Installation and initial measurement results of the Rogowski-coil-based wind turbine lightning current waveform measurement system, Electric Power Systems Research 238 (2025) 111061. https://doi.org/10.1016/j.epsr.2024.111061.

[5] F. Vukovic, B. Filipovic-Grcic, N. Stipetic, B. Franc, D. Brändlein, Correlation of Prototype Lightning Current Waveform Measurement System With LLS Data, in: 37th International Conference on Lightning Protection (ICLP), Dresden, 2024.

[6] M. Ishii, NEDO R&D Project for measures of lightning protection of wind turbines in Japan, in: International Symposium on Lightning Protection, 2015.

[7] Y. Ueda, M. Fukuda, T. Matsushuta, S. Arinaga, N. Iwai, K. Inoue, Measurement experience of lightning currents to wind turbines., Ratio (Oxf) 4 (2007).

[8] M. Miki, T. Miki, A. Wada, A. Asakawa, Y. Asuka, N. Honjo, Observation of lightning flashes to wind turbines, in: 2010 30th International Conference on Lightning Protection (ICLP), IEEE, 2010: pp. 1–7. https://doi.org/10.1109/ICLP.2010.7845869.

[9] L. Cai, Y. Ke, W. Chu, W. Liu, M. Zhou, J. Wang, Development Process of Lightning Stroke on Wind Turbine Based on High-Speed Camera Observation, in: 2022 36th International Conference on Lightning Protection (ICLP), IEEE, 2022: pp. 32–35. https://doi.org/10.1109/ICLP56858.2022.9942663.

[10] T.P. Da Silva, M.M.F. Saba, T.A. Warner, R. Alipio, C. Schumann, J.C.O. Silva, Lightning occurrence on wind turbines, Lightning Occurrence on Wind Turbines, in: 2024 International Conference on Lightning Protection (ICLP), Dresden, 2024.

[11] N. Wilson, J. Myers, K. Cummins, M. Hutchinson, A. Nag, Lightning attachment to wind turbines in central Kansas: Video observations, correlation with the nldn and in-situ peak current measurements, in: European Wind Energy Conference and Exhibition, EWEC 2013, 2013: pp. 284–291.

[12] A. Candela Garolera, K.L. Cummins, S.F. Madsen, J. Holboell, J.D. Myers, Multiple Lightning Discharges in Wind Turbines Associated With Nearby Cloud-to-Ground Lightning, IEEE Trans Sustain Energy 6 (2015) 526–533. https://doi.org/10.1109/TSTE.2015.2391013.

[13] J. Montanyà, O. van der Velde, E.R. Williams, Lightning discharges produced by wind turbines, Journal of Geophysical Research: Atmospheres 119 (2014) 1455–1462. https://doi.org/10.1002/2013JD020225.

[14] F.H. Heidler, C. Paul, High-Speed Video Observation, Currents, and EM-Fields From Four Negative Upward Lightning to the Peissenberg Tower, Germany, IEEE Trans Electromagn Compat 63 (2021) 803–810. https://doi.org/10.1109/TEMC.2020.3032781.

[15] H. Zhou, G. Diendorfer, R. Thottappillil, H. Pichler, M. Mair, Characteristics of upward bipolar lightning flashes observed at the Gaisberg Tower, J Geophys Res 116 (2011) D13106. https://doi.org/10.1029/2011JD015634.

[16] S. Visacro, M. Guimaraes, M.H. Murta Vale, Features of Upward Positive Leaders Initiated From Towers in Natural Cloud-to-Ground Lightning Based on Simultaneous High-Speed Videos, Measured Currents, and Electric Fields, Journal of Geophysical Research: Atmospheres 122 (2017). https://doi.org/10.1002/2017JD027016.

[17] F. Rachidi, M. Rubinstein, Säntis lightning research facility: a summary of the first ten years and future outlook, E & i Elektrotechnik Und Informationstechnik 139 (2022) 379–394. https://doi.org/10.1007/s00502-022-01031-2.

[18] S. Kazazi, A.M. Hussein, P. Liatos, Evaluation of NALDN performance characteristics in the vicinity of the CN Tower based on tall-structure lightning, Electric Power Systems Research 153 (2017) 19–31. https://doi.org/10.1016/j.epsr.2016.12.005.

[19] T. Miki, M. Saito, T. Shindo, M. Ishii, Current Observation Results of Downward Negative Flashes at Tokyo Skytree From 2012 to 2018, IEEE Trans Electromagn Compat 61 (2019) 663–673. https://doi.org/10.1109/TEMC.2019.2910319.

[20] M. Miki, T. Miki, A. Asakawa, T. Shindo, Characteristics of negative upward stepped leaders in positive upward lightning, in: XV International Conference on Atmospheric Electricity, 2014.

[21] Y. Yang, Z. Qiu, Z. Qin, M. Chen, Y. Du, Preliminary results of lightning current measurements at the 356 m high Shenzhen Meteorological Gradient Tower in South China, in: 2018 34th International Conference on Lightning Protection (ICLP), IEEE, 2018: pp. 1–4. https://doi.org/10.1109/ICLP.2018.8503458.

[22] X. Wang, D. Wang, J. He, N. Takagi, Characteristics of Electric Currents in Upward Lightning Flashes From a Windmill and its Lightning Protection Tower in Japan, 2005–2016, Journal of Geophysical Research: Atmospheres 126 (2021). https://doi.org/10.1029/2020JD034346.

[23] J.R. Smit, H.G.P. Hunt, C. Schumann, The Johannesburg Lightning Research Laboratory, Part 1: Characteristics of lightning currents to the Sentech Tower, Electric Power Systems Research 216 (2023) 109059. https://doi.org/10.1016/j.epsr.2022.109059.

[24] W. Xu, W. Lyu, X. Wang, L. Chen, B. Wu, Q. Qi, Ying M, Leyan H, Correlation between the Channel Discharge Current and Spectrum of a Single-Stroke Lightning Flash to Canton Tower, Remote Sensing 15(24) (2023).

[25] J.D. Hill, M.A. Uman, D.M. Jordan, T. Ngin, W.R. Gamerota, J. Pilkey, J. Caicedo, The attachment process of rocket-triggered lightning dart-stepped leaders, Journal of Geophysical Research: Atmospheres 121 (2016) 853–871. https://doi.org/10.1002/2015JD024269.

[26] J. Montanyà, J.A. López, C.A. Morales Rodriguez, O.A. van der Velde, F. Fabró, N. Pineda, J. Navarro-González, V. Reglero, T. Neubert, O. Chanrion, S.J. Goodman, N. Østgaard, A. Ladino-Rincon, D. Romero, G. Solà, R. Horta, M. Freijó, A Simultaneous Observation of Lightning by ASIM, Colombia-Lightning Mapping Array, GLM, and ISS-LIS, Journal of Geophysical Research: Atmospheres 126 (2021). https://doi.org/10.1029/2020JD033735.

[27] O.A. van der Velde, J. Montanyà, T. Neubert, O. Chanrion, N. Østgaard, S. Goodman, J.A. López, F. Fabró, V. Reglero, Comparison of High-Speed Optical Observations of a Lightning Flash From Space and the Ground, Earth and Space Science 7 (2020). https://doi.org/10.1029/2020EA001249.

[28] J. Montanyà, J.A. López, O. van der Velde, G. Solà, D. Romero, C. Morales, S. Visacro, M.M.F. Saba, S.J. Goodman, E. Williams, M. Peterson, N. Pineda, M. Arcanjo, D. Aranguren, Potential use of space-based lightning detection in electric power systems, Electric Power Systems Research 213 (2022) 108730. https://doi.org/10.1016/j.epsr.2022.108730.

[29] IEC, Wind energy generation systems-Part 24: Lightning protection (No. 61400-24), 2019.

[30] J. Montanyà, Fabró, F., van der Velde, O., March, V., Williams, E. R., Pineda, N., Romero, D., Solà, G., and Freijo, M.: Global distribution of winter lightning: a threat to wind turbines and aircraft, Nat. Hazards Earth Syst. Sci., 16, 1465-1472, doi:10.5194/nhess-16-1465-2016, 2016

[31] J. Montanyà, A.R. Jara-Jiménez, O. van der Velde, J.A. López, N. Pineda, J. López, S. Vogel, S.F. Madsen, S. M. Steiger, E. C. Bruning, V. C. Chmielewski, J. Trostel and J.Losego (2024), Upward flashes to wind turbines during winter observed from space by ISS-LIS and GLM, 37th International Conference on Lightning Protection (ICLP 2024), pp. 1026-1031, 1-7 September, 2024, Dresden,)Germany).

[32] M. Bateman, Mach, D., & Stock, M. (2021). Further investigation into detection efficiency and false alarm rate
for the geostationary lightning mappers aboard GOES-16 and GOES-17. Earth and Space Science, 8, 2020EA001237. https://doi.org/10.1029/2020EA001237

[33] J. Montanyà, et al. (2024). Analysis of the MTG Lightning Imager performance during the first days of public data with the Ebro Lightning Mapping Array and the ASIM instrument on the ISS, 2024 AGU Annual Meeting, AE32A-01, Washington DC, USA.

[34] C. Schumann, M.M.F. Saba, T.A. Warner, et al. (2019). On the triggering mechanisms of upward lightning Sci. Rep., 9 (2019), p. 9576, 10.1038/s41598-019-46122-x

[35] O. A. Van Der Velde and J. Montanyà, "Asymmetries in bidirectional leader development of lightning flashes," Journal of Geophysical Research Atmospheres, 2013, doi: 10.1002/2013JD020257.

[36] R. Stuhlmann, A. Rodriguez, S. Tjemkes, J. Grandell, A. Arriaga, J.-L. Bézy, D. Aminou, P. Bensi,Plans for EUMETSAT's third generation meteosat geostationary satellite programme, Adv. Space Res., 36 (5) (2005), pp. 975-981

[37] Krehbiel, P. R., Brook, M. & McCrory, R. A. An analysis of the charge structure of lightning discharges to ground. J. Geophys. Res. 84, 2432-2456 (1979).